Beta Conjunction Analysis Tool

Salvatore Alfano*
Center for Space Standards and Innovation, Colorado Springs, Colorado, 80920

A means for testing some upcoming new features in Satellite Tool Kit's Advanced Close Approach Tool is presented. Given two conjuncting objects' positions, velocities, and covariances, assessments are made for both linear and non-linear relative motion. For the former, true and maximum probabilities are computed as well as the probability dilution region. A fractional probability threshold is then defined based on a user's accuracy requirement and the minimum relative velocity found that ensures sufficient linearity. A coarse determination of this velocity is made by forcing the relative motion to be linear but allowing the covariance to vary with time. This is followed by a refined estimate where orbital dynamics are included for the trajectory motion. Nonlinear probability is computed by breaking the collision tube into sufficiently small tubes such that the sectional motion is nearly linear, computing the linear probability associated with each section, and then summing. Two approaches are taken to determine the nonlinear probability. The first considers each tube to be cylindrical, with its ends perpendicular to its axis; this does not account for gaps or overlaps of abutting cylinders. The second is more complex, using bundled, rectangular parallelepipeds to eliminate these gaps and overlaps by treating the junctions as compound miters while incorporating probability density variations. The objects are treated as spheres for testing, but the complex nonlinear method is designed to handle any time-varying object shape by using dynamic pixel files of the object images.

Nomenclature

C	=	covariance matrix
erf	=	error function
f	=	fractional probability threshold (or aspect ratio)
F	=	6x6 position/velocity Jacobian matrix
M_f	=	final Mahalanobis distance
M_i	=	initial Mahalanobis distance
n	=	covariance ellipsoid scale factor
OBJ	=	cross-sectional radius
P	=	probability
R	=	radius of torus
TCA	=	time of closest approach
xm	=	rotated x position of combined object center
ym	=	rotated y position of combined object center
α	=	angle between the object's distance vector and the covariance ellipse's x axis
Δt	=	transition time
ε	=	covariance-centric angle
μ	=	gravitational parameter
ϕ	=	object-centric angle in Mahalanobis space
Φ	=	state transition matrix
ρ	=	combined object radius
σ	=	standard deviation
τ	=	unitized parameter for time
θ	=	object-centric angle

* Senior Research Astrodynamicist, CSSI, 7150 Campus Drive, Suite 260, Colorado Springs, CO, 80920-6522, salfano@centerforspace.com, AIAA Associate Fellow.

I. Introduction

Many of the assumptions involved in linear collision probability formulation[1-8] are eliminated in this paper. Typically, space object collision probability analysis (COLA) is conducted with the objects modeled as spheres, thus eliminating the need for attitude information. Their relative motion is considered linear for the encounter by assuming the effect of relative acceleration is dwarfed by that of the velocity. The positional errors are assumed to be zero-mean, Gaussian, uncorrelated, and constant for the encounter. The relative velocity at the point of closest approach is deemed sufficiently large to ensure a brief encounter time and static covariance. The probability of collision P is defined as the integral of the probability density function over the swept-out volume (collision tube) V

$$P = \frac{1}{\sqrt{8\cdot\pi^3}\cdot|C3|}\cdot\int\int_{V}\int e^{\frac{-1}{2}\cdot r^T\cdot C3^{-1}\cdot r}\,dx\,dy\,dz \tag{1}$$

where C3 is the positional covariance matrix and r is the relative distance vector between the two objects[12]. Coupled with object sizes, the encounter region determines the limits of integration. The region is defined when one object is within a standard deviation (σ) combined covariance ellipsoid shell scaled by a factor of n. This user-defined, three-dimensional, n-σ shell is centered on the primary object; n is typically in the range of 3 to 8 to accommodate conjunction possibilities ranging from 97.070911% to 99.999999%.

The assumption of linear relative motion may not be valid in all cases. Chan[6] proposed test criteria for nonlinearity. Chan[9], Patera[10], Alfano[11], and McKinley[12] proposed different methods for calculating collision probability for such instances. Nonlinear motion is typically associated with long-term encounters which imply the covariance can no longer be assumed static. The collision tube will not be straight, invalidating the simple dimensional reduction used for linear motion. The size of the n-σ shell must also be carefully considered, especially if the relative motion reverses direction during the encounter.

This paper presents a method to determine when the linear relative motion assumption is valid by determining the minimum relative velocity needed at the time of closest approach (TCA). This velocity ensures a pre-specified probability difference will not be exceeded either forward or backward in time. The process uses a coarse assessment to bound the problem and then a refined assessment that uses the full force models to predict relative orbital motion and covariance changes. If the actual relative velocity exceeds the minimum, then the linear assumption is valid for the encounter.

Should the relative motion be deemed nonlinear, then two methods are presented to compute probability. The first method adjoins right cylinders (tubes) in Cartesian space. For each time step the tube sections are sufficiently small enough so that, over the interval, the relative motion can be assumed linear and the covariance constant. At every time step the objects, their positions, and their covariances are transformed to the Mahalanobis space and the tube section probability calculated. To address object distortion due to Mahalanobis transformation, a computationally efficient probability engine for elliptical shapes is presented. This approach may produce gaps and overlaps where the tube sections meet.

The second method eliminates these gaps and overlaps, applies to all relative motion, and is coupled with a modified error-function method to accommodate any object shape. Each tube section is represented by a bundle of abutting parallelepipeds of differing lengths to create a compound miter with the neighboring tube. At every time step the parallelepipeds are transformed to the Mahalanobis space and their probabilities determined using error functions. This method is somewhat similar to the more time-consuming voxel[11] method. In essence the voxels are no longer cubes with constant dimensions in Mahalanobis space; they are extended along the relative velocity vector to create parallelepipeds that can be resized and reoriented for each tube section. Given the pixel file of each object as seen along the relative velocity vector, these files can be merged. Each pixel in the merged file that contains a segment of the combined object becomes the face of another parallelepiped. Thus, any object shape can be readily accommodated without modifying the probability integrand by simply omitting or including certain parallelepipeds.

The aforementioned methods are scripted in MATLAB. The tool can read inputs from the STK data provider or an EXCEL spreadsheet and employs a Graphical User Interface (GUI). The interface has default values for all intermediate and final computational variables that the user may interactively change for analysis.

II. Testing for Linear Relative Motion

For linear relative motion, the probability along the relative velocity vector (collision tube) is conveniently removed from the calculations. For nonlinear relative motion, that dimension must be reintroduced. Two consecutive tests are developed here to determine when the relative motion is sufficiently linear to assume the former. This is done by finding the minimum relative velocity needed at the time of closest approach (TCA) to ensure a pre-specified probability difference will not be exceeded either forward or backward in time while the n-σ shell is traversed. The user defines a fractional probability threshold (f) that is within accuracy requirements for intended operations; f is the absolute difference between the linear and nonlinear results divided by the linear results. Initially a coarse assessment is performed only on the covariance growth using simple, two-body, orbital dynamics to approximate the bounds of linear motion based on the threshold f. This bounding is followed by a refined assessment using the full force models to predict relative orbital motion and covariance changes. The minimum relative velocity is then determined to ensure the fractional probability threshold will not be exceeded. The linear assumption is valid if the encounter's relative velocity exceeds the minimum.

A. Coarse Assessment

For the bounding assessment, the relative motion is treated as linear but the covariance is allowed to grow using the primary object's simple two-body dynamics. The assessment begins with the objects' positions, velocities, and covariance data at TCA (t=0). The examination region is bounded by the user specifying the size of the n-σ shell that must be traversed. An initial estimate of time change Δt_{init} is made by dividing the distance to traverse n-σ by the magnitude of relative velocity. Beginning and end times (t_{start}, t_{end}) are preliminarily determined by using the relative velocity at time of closest approach and holding the n-σ shell static to determine entry and exit. The next step is to compute the linear probability at TCA, P(TCA). This method is not limited to a specific two-dimensional probability model. For this paper, a simple form of Chan's analytical probability approximation[4] (P_S1) is used

$$P\_S1 = \exp\left[\frac{-1}{2}\cdot\left(\frac{xm^2}{\sigma x^2}+\frac{ym^2}{\sigma y^2}\right)\right]\cdot\left[1-\exp\left[\frac{-1}{2}\cdot\left(\frac{OBJ^2}{\sigma x\cdot\sigma y}\right)\right]\right] \tag{2a}$$

where the encounter plane axes are aligned with the 2x2 covariance axes in Cartesian space to eliminate cross-correlation terms. After determining and applying the appropriate rotation matrix, the combined object radius OBJ is centered at (xm, ym) with associated standard deviations of (σx, σy). The first parenthetical expression in Equation 1a is recognized as the mahalanobis miss distance squared and the second as the mahalanobis equivalent object area. With this recognition, an equivalent form of Equation 1a is presented where the encounter plane axes need not be aligned with the covariance axes, thus eliminating the computational burden of rotation.

$$P\_S1 = \exp\left[\frac{-1}{2}\cdot\left[(x\ \ y)\cdot C2^{-1}\cdot\begin{pmatrix}x\\y\end{pmatrix}\right]\right]\cdot\left[1-\exp\left[\frac{-1}{2}\cdot\left(\frac{OBJ^2}{\sqrt{|C2|}}\right)\right]\right] \tag{2b}$$

By assuming linear relative motion coupled with a dynamic covariance, the combined object center remains fixed at (x, y) and the 2x2 combined covariance C2 is the only parameter that changes with time. These expressions were chosen for their simplicity and computational rapidity[8].

Simple covariance propagation is accomplished using a point mass model. In Cartesian space, the primary object is located at the earth-centered position (x_p, y_p, z_p). The gravitational parameter is μ, the primary's radial distance is r, and the time shift from TCA is dt. The 6x6 covariance state transition matrix is approximated by

$$\Phi 6 = I6 + F\cdot dt\cdot\left(I6 + F\cdot\frac{dt}{2}\right) \tag{3}$$

where I6 is the 6x6 identity matrix and F is the two-body Jacobian matrix[13]

$$F = \begin{bmatrix} 0 & 0 & 0 & 1 & 0 & 0 \\ 0 & 0 & 0 & 0 & 1 & 0 \\ 0 & 0 & 0 & 0 & 0 & 1 \\ \frac{-\mu}{r^3} + \frac{3\cdot\mu}{r^5}\cdot\left(x_p\right)^2 & \frac{3\cdot\mu}{r^5}\cdot x_p\cdot y_p & \frac{3\cdot\mu}{r^5}\cdot x_p\cdot z_p & 0 & 0 & 0 \\ \frac{3\cdot\mu}{r^5}\cdot x_p\cdot y_p & \frac{-\mu}{r^3} + \frac{3\cdot\mu}{r^5}\cdot\left(y_p\right)^2 & \frac{3\cdot\mu}{r^5}\cdot y_p\cdot z_p & 0 & 0 & 0 \\ \frac{3\cdot\mu}{r^5}\cdot x_p\cdot z_p & \frac{3\cdot\mu}{r^5}\cdot y_p\cdot z_p & \frac{-\mu}{r^3} + \frac{3\cdot\mu}{r^5}\cdot\left(z_p\right)^2 & 0 & 0 & 0 \end{bmatrix}. \quad (4)$$

Only the positional 3x3 covariance is needed for the probability calculation. This allows the dimensionality of the covariance state transition matrix to be reduced to a 3x6

$$\Phi(dt) = \begin{pmatrix} 1 & 0 & 0 & dt & 0 & 0 \\ 0 & 1 & 0 & 0 & dt & 0 \\ 0 & 0 & 1 & 0 & 0 & dt \end{pmatrix} + \frac{dt^2}{2}\cdot\left[\begin{pmatrix} 1 & 0 & 0 & 0 & 0 & 0 \\ 0 & 1 & 0 & 0 & 0 & 0 \\ 0 & 0 & 1 & 0 & 0 & 0 \end{pmatrix}\cdot\frac{-\mu}{r^3} + \begin{bmatrix} \left(x_p\right)^2 & x_p\cdot y_p & x_p\cdot z_p & 0 & 0 & 0 \\ x_p\cdot y_p & \left(y_p\right)^2 & y_p\cdot z_p & 0 & 0 & 0 \\ x_p\cdot z_p & y_p\cdot z_p & \left(z_p\right)^2 & 0 & 0 & 0 \end{bmatrix}\cdot\frac{3\cdot\mu}{r^5}\right]. \quad (5)$$

Positional covariance (C3) is then determined from the 6x6 covariance (C6) at TCA as

$$C3(dt) = \Phi(dt)\cdot C6(TCA)\cdot\Phi(dt)^T \quad (6)$$

Using the data at TCA, constant relative velocity is assumed and the relative position computed for t_{start}. If desired, each object's covariance can be propagated to t_{start} using Equations 5 and 6 and then summed; obviously the positional values in Equation 5 would be modified for the secondary object. Because this is only a coarse assessment and the objects are very near each other, $\Phi(dt)$ will be nearly identical for both, This allows a simpler and faster propagation of the combined covariance to t_{start} in a single step using Equations 5 and 6. This data is then used to find the associated probability at t_{start} , $P(t_{start})$. If the fractional tolerance between P(TCA) and $P(t_{start})$ is exceeded then t_{start} is assigned half its previous value and the process repeated until within the tolerance. When completed, t_{start} becomes an initial estimate for how quickly the n-σ shell must be traversed from TCA for the conjunction to be considered linear. The same process is repeated for t_{end}. If the start and end times remain unchanged from their initial values, the user might consider stopping here and assume linear motion using P(TCA) for the encounter probability.

B. Refined Assessment

Given $P(t_{start})$, P(TCA), and $P(t_{end})$ from the coarse assessment and realizing that the P curve is convex[14], a quadratic curve fit is employed to more closely associate the start and end times with the fractional probability tolerance. A new initial estimate for how quickly the n-σ shell must be traversed from TCA is found by halving the difference between the fitted start and end times to produce Δt_{coarse}. A coarse assessment of the minimum relative velocity needed to satisfy the fractional tolerance is determined by scaling the TCA relative velocity by $\Delta t_{init}/\Delta t_{coarse}$. The secondary object's velocity is then modified to reflect this; the choice of modifying the primary

or secondary is arbitrary. These new times and this new velocity are used with complex orbital force models to propagate positions and covariances from TCA to find the associated $P(t_{start})$ and $P(t_{end})$. A quadratic curve fit is again employed to refine the traversal time and produce Δt_{fine}. The minimum relative velocity needed is recomputed by scaling the original relative velocity by $\Delta t_{init}/\Delta t_{fine}$.

To accomplish this, the unitized parameter τ is computed from a quadratic curve fit as follows

$$dP = f \cdot P(TCA) \tag{7a}$$

$$dP = -f \cdot P(TCA) \quad \text{if} \quad \max\left(P\left(t_{start}\right), P\left(t_{end}\right)\right) < P(TCA) \tag{7b}$$

$$\tau = \min\left[\left|\frac{P\left(t_{end}\right) - P\left(t_{start}\right) + \sqrt{\left|\left(P\left(t_{end}\right) - P\left(t_{start}\right)\right)^2 - \left(2 \cdot P(TCA) - P\left(t_{end}\right) - P\left(t_{start}\right)\right) \cdot (8 \cdot dP)\right|}}{2 \cdot \left(2 \cdot P(TCA) - P\left(t_{end}\right) - P\left(t_{start}\right)\right)}\right|, \left|\frac{P\left(t_{end}\right) - P\left(t_{start}\right) - \sqrt{\left|\left(P\left(t_{end}\right) - P\left(t_{start}\right)\right)^2 - \left(2 \cdot P(TCA) - P\left(t_{end}\right) - P\left(t_{start}\right)\right) \cdot (8 \cdot dP)\right|}}{2 \cdot \left(2 \cdot P(TCA) - P\left(t_{end}\right) - P\left(t_{start}\right)\right)}\right|\right] \tag{8}$$

The coarse assessment data is inserted into the above equations to find Δt_{coarse}

$$\Delta t_{coarse} = \frac{\left|\left(\tau^2 - \tau\right) \cdot t_{end} + \left(\tau^2 + \tau\right) \cdot t_{start}\right|}{2} \tag{9}$$

The original relative velocity is scaled by $\Delta t_{init}/\Delta t_{coarse.}$ and the secondary object's velocity modified to reflect this. End and start times are reset to +/– Δt_{coarse} . $P(t_{start})$ and $P(t_{end})$ are recomputed from TCA using the secondary's modified velocity and complex orbital force models to propagate positions and covariances. Equations 7 and 8 are employed again to produce a new τ which produces a refined Δt as follows

$$\Delta t_{fine} = \tau \cdot \Delta t_{coarse} \tag{10}$$

The approximate, minimum, relative velocity needed to ensure sufficient linearity is finally determined by scaling the original relative velocity by $\Delta t_{init}/\Delta t_{fine.}$. This new velocity is consistent with the linear assumptions based on the user-defiend fractional probability threshold. If the encounter's relative velocity equals or exceeds this minimum, then the linear assumption holds. If not, then a probability method that does not assume linear relative motion should be used.

The minimum relative velocity could also be found by repeated sampling and adjusting but would be more time consuming. It is this author's opinion that determining the exact velocity that is consistent with the linearity assumptions would require more processing than simply computing the nonlinear conjunction probability itself.

III. Method of Adjoining Tubes

This nonlinear probability method[10,11] begins with object position, velocity, and covariance data at TCA. Propagation is done forward/backward in time until a user limit is reached. For each time step the tube sections are modeled as right cylinders that are sufficiently small enough so that, over the interval, the relative motion can be

assumed linear and the covariance constant. At every time step the objects, their positions, and their covariances are transformed to the Mahalanobis space. For each tube section, a two-dimensional probability P_{2d} is computed by projecting the combined object shape onto a plane perpendicular to the relative velocity. In addition, a one-dimensional probability is computed along the relative velocity vector by using each endpoint's Mahalanobis distance. The cylinder endpoints (M_i, M_f) are used to compute long-axis probability P_{1d} from

$$P_{1d} = \left| \frac{1}{2} \cdot \left(\operatorname{erf}\left(\frac{M_f}{\sqrt{2}} \right) - \operatorname{erf}\left(\frac{M_i}{\sqrt{2}} \right) \right) \right| \tag{11}$$

The product of P_{1d} and P_{2d} yields the sectional probability of each tube. All sectional probabilities are summed until the user limit is reached. To accommodate the elliptical object footprint in the Mahalanobis encounter plane, Equation 1a can be used to find P_{2d} provided the equivalent object area assumption is deemed adequate. One can also use existing two-dimensional probability methods that assume a circular footprint by rescaling the space to make the object circular again. Patera[7] derived an expression that can incorporate any shape but requires reformulating the integrand. As an alternative, a probability model that uses an approach similar to Patera's is developed here for computing P_{2d} while remaining in Mahalanobis space.

One of the challenges when working in Mahalanobis space is the combined object distortion that results from rescaling the combined positional covariance to have unit variance along each dimension. The transformation is accomplished by determining the eigenvalues and associated eigenvectors of the combined positional covariance matrix. The eigenvectors are used to reorient all data while diagonalizing the covariance. All data is then scaled using the corresponding eigenvalues so that the covariance matrix becomes the identity matrix. The spherical object in Cartesian space becomes an ellipsoid, the circle an ellipse. The method of adjoining tubes requires a two-dimensional probability calculation for each segment, but in this space the object footprint may no longer be circular.

Patera reduced the two-dimensional probability integral to a one-dimensional path integral where r is the distance to the hardbody perimeter and ε is the covariance-centric angular position measured from the x-axis. The probability density is symmetrized to produce the expression

$$P = \frac{1}{2 \cdot \pi} \oint_{\text{perimeter}} \left(1 - \exp\left(\frac{-r^2}{2 \cdot \sigma^2} \right) \right) d\varepsilon \tag{12}$$

where P is the collision probability, σ is the symmetrized position error standard deviation (σ_x), and the angle ε is covariance-centric. The details for computing r can be found in Patera's 2001 paper[3].

In a subsequent 2005 Engineering Note[7] Patera switched the integration variable to center it on the object. He oriented the frame to place the combined object center at (R, 0) with α defining the angle between the object's distance vector and the covariance ellipse's x axis. He again symmetrized the space using σ_x. and defined θ as the object-centric angle. The reformulation reduced intermediate complexities and also resulted in substantially fewer integration steps to achieve a given level of accuracy. This improved, object-centric method is expressed in integral form as

$$P = \frac{1}{2 \cdot \pi} \cdot \int_0^{2 \cdot \pi} \left(\frac{f \cdot \rho^2 + R \cdot f \cdot \rho \cdot \cos(\theta) + R \cdot f \cdot \frac{d\rho}{d\theta} \cdot \sin(\theta)}{r^2} \right) \cdot \left(1 - \exp\left(\frac{r^2}{2 \cdot \sigma^2} \right) \right) d\theta \tag{13}$$

where ρ is the combined object radius, f is the ratio of the covariance matrix's σ_x to σ_y, and r^2 is expressed as

$$r^2 = \left(R + \rho\cdot\cos(\theta)\right)^2\cdot\left(\cos(\alpha)^2 + f^2\cdot\sin(\alpha)^2\right) + \rho^2\cdot\sin(\theta)^2\cdot\left(\sin(\alpha)^2 + f^2\cdot\cos(\alpha)^2\right)$$

$$+ \ 2\cdot\rho\cdot\left(1 - f^2\right)\cdot\cos(\alpha)\cdot\sin(\alpha)\cdot\sin(\theta)\cdot\left(R + \rho\cdot\cos(\theta)\right) \quad . \tag{14}$$

Simple numerical methods require only two sine and two cosine evaluations regardless of the number of integration steps. The method is accurate and efficient and has been has been shown[8] to produce results with less than one percent error in 50 integration steps or less. If the object is circular then ρ is constant ($d\rho/d\theta = 0$). If it is elliptical, evaluating the expression becomes more complicated.

Following a derivation similar to Patera's, further simplification can be achieved through a different axes alignment and symmetrization. Aligning the Cartesian frame with the covariance ellipse's axes and subsequently symmetrizing to unity, the probability equation is recast in Mahalanobis space. The f term in Patera's formulation does not appear because the standard deviations in this space all equal one. The sizes of the now-elliptical object's x and y axes become ρ_x and ρ_y with its center located at (x_maha, y_maha). After much manipulation, the expression representing the two-dimensional probability integral P_{2d} becomes

$$P_{2d} = \frac{\rho_x\cdot\rho_y}{2\cdot\pi}\cdot\int_0^{2\cdot\pi} \frac{1 + \frac{x\_maha}{\rho_x}\cdot\cos(\phi) + \frac{y\_maha}{\rho_y}\cdot\sin(\phi)}{\left(\rho_x\cdot\cos(\phi) + x\_maha\right)^2 + \left(\rho_y\cdot\sin(\phi) + y\_maha\right)^2}\cdot\left[1 - \exp\left[\frac{-\left[\left(\rho_x\cdot\cos(\phi) + x\_maha\right)^2 + \left(\rho_y\cdot\sin(\phi) + y\_maha\right)^2\right]}{-2}\right]\right] d\phi \tag{15}$$

In series form this can be represented as

$$P_{2d} = \frac{\rho_x\cdot\rho_y}{n}\cdot\sum_{i=1}^{n}\left[\left(1 + \frac{x\_maha}{\rho_x}\cdot\cos\left(\frac{i\cdot 2\cdot\pi}{n}\right) + \frac{y\_maha}{\rho_y}\cdot\sin\left(\frac{i\cdot 2\cdot\pi}{n}\right)\right)\cdot maha\_term(i)\right] \tag{16a}$$

$$maha\_term(i) = \frac{1}{maha\_sqrd(i)}\cdot\left(1 - \exp\left(\frac{maha\_sqrd(i)}{-2}\right)\right) \tag{16b}$$

$$maha\_sqrd(i) = \left(\rho_x\cdot\cos\left(\frac{i\cdot 2\cdot\pi}{n}\right) + x\_maha\right)^2 + \left(\rho_y\cdot\sin\left(\frac{i\cdot 2\cdot\pi}{n}\right) + y\_maha\right)^2 \tag{16c}$$

Simple numerical methods require only one sine and one cosine evaluation for the entire series regardless of n. Should maha_sqrd be close to zero, then a fifth-order series expansion of Equation 15b in terms of maha_sqrd is sufficient. As with Patera's 2005 method, this is accurate, efficient, and produces the same results as Equation 13. The advantage is that the object footprint is now conveniently represented as an ellipse in Mahalanobis space.

For comparison, in this transformed space Equation 2a becomes

$$P\_S1 = \exp\left[\frac{-1}{2}\cdot\left(x\_maha^2 + y\_maha^2\right)\right]\cdot\left[1 - \exp\left[\frac{-1}{2}\cdot\left(\rho_x\cdot\rho_y\right)\right]\right] \tag{17}$$

The gaps and overlaps where the tube sections meet can cause the probability to be somewhat under- or over-estimated. If the relative motion track bends towards the covariance ellipsoid center, then the overlapping sections will occur in regions of greater probability density with the gaps occurring in regions of lesser probability density. Although the gap and overlapping volumes are almost equal, the resulting summation causes an over-inflation of the

probability. If the relative motion track bends away from the covariance ellipsoid center, then the probability for cylindrical tubes will be underestimated because the gap is in a region of higher probability density. The amount of error will vary based on the degree of bending/overlap relative to probability density. Incremental limits of 100 seconds for maximum time step, one degree for maximum acceptable angle between adjoining tubes, and 0.25 σ for the maximum change in long-axis sigma for any tube were sufficient to achieve at least two significant figures of accuracy when calculating probability[11].

IV. Method of Adjoining Parallelepipeds

The right cylinders described in the previous section are replaced by bundles of abutting parallelepipeds. Each parallelepiped end is adjusted to form a compound miter where neighboring tubes meet, thereby eliminating any gaps or overlaps. The approach that follows applies to all relative motion and is coupled with a modified error-function method[5] to allow any object shape. As before the method begins with object position, velocity, and covariance data at TCA. Propagation is done forward/backward in time until a user limit is reached. For each time step the tube sections are sufficiently small enough so that, over the interval, the relative motion can be assumed linear and the covariance constant. The probability of each parallelepiped is computed and summed to obtain the overall probability of the tube section. All sections are summed to produce the overall encounter probability.

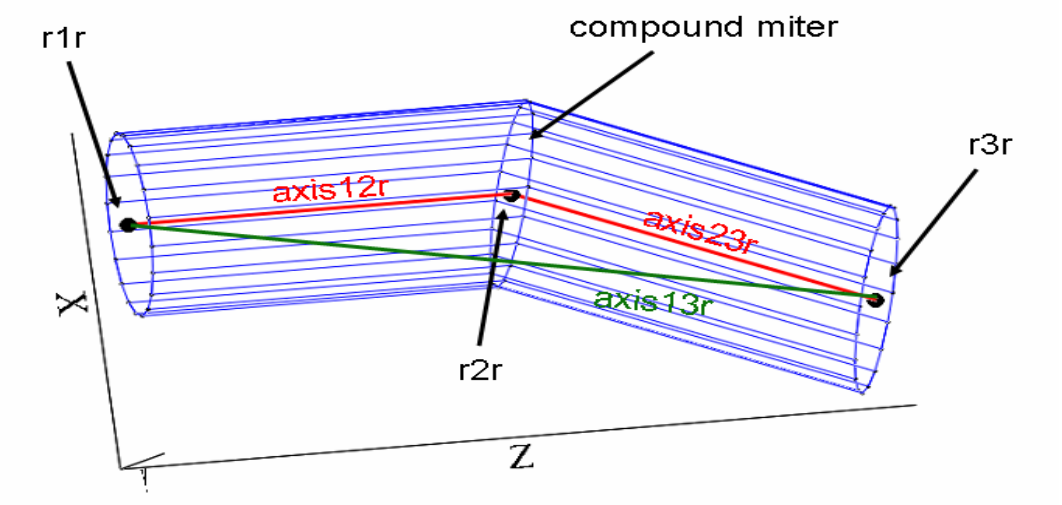

Figure 1. Compound miter description.

Geometric projections determine the end points of each parallelepiped. Let r1, r2, and r3 be three consecutive points along the relative trajectory. Determine the unit vectors from r1 to r2 (axis12 for the first tube) and r2 to r3 (axis23 for the second tube). Rotate the axes to a new frame (denoted by suffix r) where the z component is aligned with axis12 such that after rotation axis12r is (0 0 1) as shown in Figure 1. Define axis13r as the sum of axis12r and axis23r; the compound miter is perpendicular to axis13r and passes through r2r. In the new frame the r2r end point adjustment dz for each parallelepiped is found by examining the first tube's off-axis positions dx and dy through the equation

$$dz = \frac{dx \cdot axis13r_x + dy \cdot axis13r_y}{-axis13r_z} \quad . \tag{18}$$

The use of trigonometric functions and their associated sign rectifications[12] are not needed. The center of the parallelepiped's face is shifted from r2r by (dx dy dz), placing it on the surface of the compound miter.

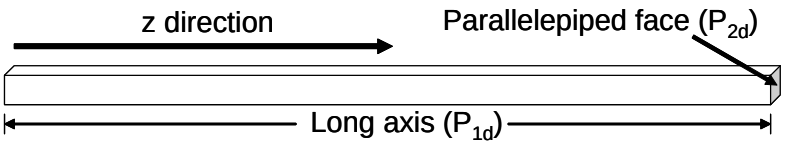

Figure 2. Parallelepiped description.

At every time step the two-dimensional probability P_{2d} is computed by aligning the parallelepiped sides with the projected covariance axes (face in Figure 2). This eliminates covariance cross-correlation terms so that Equation 11 can be used for each of the two axes individually and the results multiplied to produce P_{2d}. The parallelepiped ends as determined by Equation 17 are transformed to the Mahalanobis space and Equation 11 used to compute the long-axis probability P_{1d}. This modified error-function method[6] is somewhat similar to the more time-consuming voxel method[11]. In essence the voxels are no longer cubes with constant dimensions in Mahalanobis space; they are extended along the relative velocity vector to create parallelepipeds that can be resized and reoriented for each tube section.

Because of the approach taken to produce P_{2d}, this method can accommodate any complex object shape (convex, concave, spiral, hollow, etc.). Using the Area Tool (Ref) in STK or a similar product, a pixel file can be created for each object as seen along the relative velocity vector. These pixel files are then merged to produce a combined file that maps out all points where the two objects could touch. Each pixel that contains a segment of the combined object becomes the face of another parallelepiped and is included in the calculation.

V. Bundled Parallelepiped Implementation

Three-dimensional position and velocity data of each object, as well as their 6x6 covariance matrices, are required with the assumption that all starting data are in the Earth Centered Inertial (ECI) frame. Suitable incremental limits should be set for each time step with the user specifying the computational stopping condition in terms of time limit and/or encounter region. The computational algorithm is as follows.

Initially propagate all to Time of Closest Approach (TCA) in Earth Centered Inertial (ECI) frame
- Determine relative position r1 by propagating back one time step from TCA
- Assign original relative position to r2
- Determine relative position r3 by propagating forward one time step from TCA

Begin iteration
- Propagate forward one time step from r3 to determine relative position r4
- Create unit vector from r1 to r2, label it axis12
- Create unit vector from r2 to r3, label it axis23
- Create unit vector from r3 to r4, label it axis34
- Create vector from summation of axis12 and axis 23, label it axis13
- Create vector from summation of axis23 and axis 34, label it axis24
- Compute necessary rotation matrix to align new z component with relative velocity (axis23) while simultaneously decoupling new x and y components with respect to projected covariance.
- Rotate r2, r3, axis23, axis13, axis24, and 3x3 positional covariance (C3) associated with r2 to new frame denoting rotated data with an r suffix (r2r, r3r, axis23r, axis13r, axis24r, C3r)
- Compute necessary rotation/scaling matrix to go from new frame to Mahalanobis space where the z component is aligned with the relative velocity vector, label it T_maha
- Middle cylinder axis endpoints are r2r and r3r: [xm, ym, zm2]=r2r & [xm, ym, zm3]=r3r
  - Find z component of parallelepiped's axis ends using T_maha transformation, label them zm_start & zm_end
- For each pixel of combined object
  - Determine its width, height, and off-axis central position (dx, dy)
  - Use r2r, axis13r, dx and dy to find dz2 to define one end of parallelepiped [xm+dx, ym+dy, zm2-dz2]
  - Find z component of parallelepiped end using T_maha transformation, label it z_start

- Use r3r, axis24r, dx and dy to find dz3 to define other end of parallepiped [xm+dx, ym+dy, zm2-dz3]
- Find z component of parallelepiped end using T_maha transformation, label it z_end
- Find parallelepiped's 2D probability (face) centered at [xm+dx, ym+dy] using width and height
- Find parallelepiped's 1D probability (length) using z_start and z_end
- If sign(zm_end-zm_start) is opposite of sign(z_end-z_start) then there is overlap
  - Negate parallelepiped's 1D probability
- Multiply 1D and 2D probabilities and add to running sum

- Reassign r2 to r1, r3 to r2, r4 to r3
- Repeat until final limit reached (time, number of orbits, encounter shell limit, . . .)

This iterative procedure must be done twice, once forward in time from TCA and once backward in time.

If the time step is too large, the parallelepipeds may not adequately represent the path of the combined objects through the changing probability density space. Also, fidelity increases with the number of parallelepipeds used to represent the combined object's shape.

VI. MATLAB tool

A Beta tool was scripted in MATLAB for testing conjunctions of spherical objects. The tool can read data from the STK data provider or an Excel spreadsheet containing positions, velocities, object sizes, and 6x6 covariance matrices of both objects at TCA. The user can modify object radius directly from the Graphical User Interface (GUI) as shown in the upper left hand boxes of Figure 3.

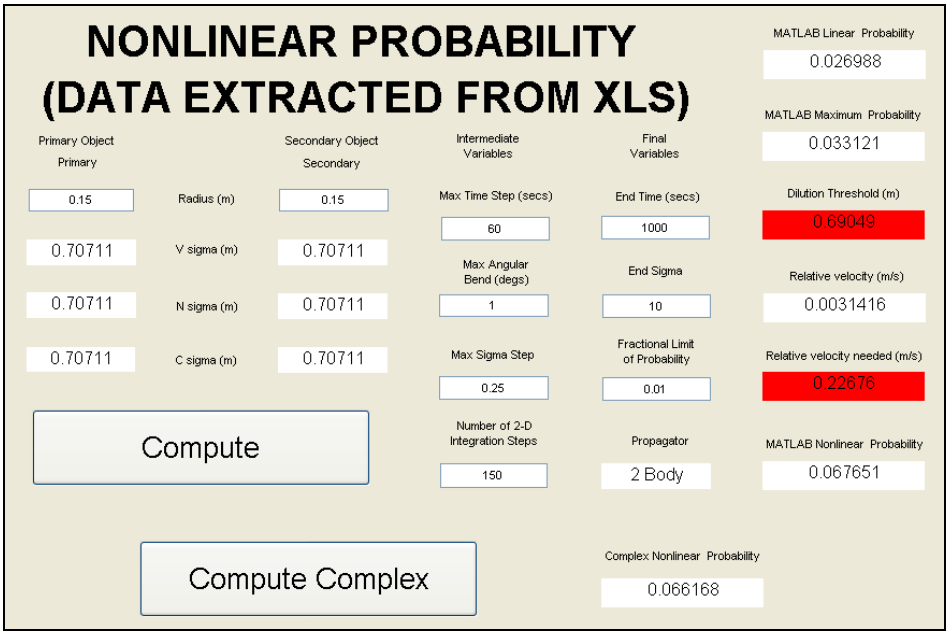

Figure 3. MATLAB Beta Tool Graphical User Interface.

The user should specify the intermediate and final variables if different from the default (recommended) settings. For the intermediate variables the Maximum Time Step sets the time step upper limit, the Maximum Angular Bend limits the angular difference between abutting cylinders, the Maximum Sigma Step limits individual cylinder length based on the traversed Mahalanobis distance, and the Number of 2-D Integration Steps defines the granularity of the two-dimensional probability computation. Calculation continues until one of the limits defined by the final variables is reached. Those limits are End Time and End Sigma. The End Sigma is the final Mahalanobis distance and also the value of n for the n-σ shell.

The Compute button generates all the results seen on the far right side of Figure 3. The beta tool computes linear and maximum probability as well as the dilution threshold[14]. If the dilution threshold is exceeded the box becomes red; if the combined covariance is adequate the box is green. The coarse and refined assessments produce the

relative velocity needed. The box is green if the actual relative velocity exceeds this, else it is red. Finally the nonlinear probability for the adjoining tubes is computed and displayed.

The Compute Complex button generates the probability using adjoining parallelepipeds. This button was constructed separately because the computation can be time consuming and possibly unnecessary based on the linearity test results.

Initial testing was done by comparing the method to linear cases and Patera's nonlinear cases. As expected, the methods matched the linear cases. For the nonlinear toroidal[10] case a circular, relative trajectory is chosen with a spherical hardbody radius and symmetric covariance ellipsoid. The object creates a torus as it follows the circular trajectory. The exact solution to collision probability was derived by Chan[9] as

$$p = \frac{2}{\sigma}\cdot\sqrt{\frac{2}{\pi}}\cdot\exp\left[\frac{-\left(R^2+r^2\right)}{2\cdot\sigma^2}\right]\cdot\int_0^r \sinh\left(\frac{R\cdot\sqrt{r^2-x^2}}{\sigma^2}\right)dx \tag{19}$$

where σ is the standard deviation, R is the torus radius, and r is the cross-sectional radius as shown in Figure 4. The collision tube is more closely represented as the number of cylinders increases. With σ set to one, R set to one, and r set to 0.3, Equation 19 produces a probability of 0.066144. The number of adjoining cylinders was varied from 4 to 100 to assess convergence behavior as displayed in the following figure.

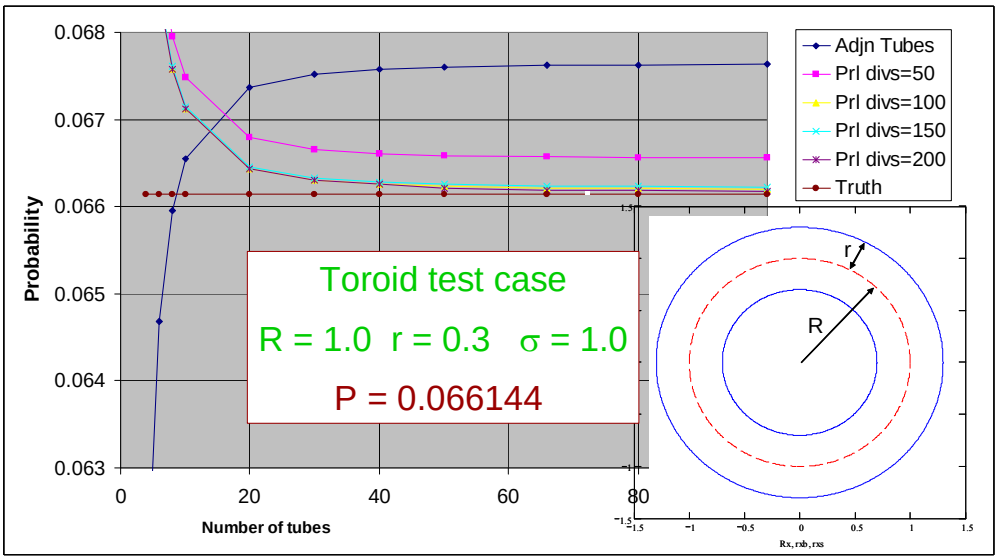

Figure 3. Circular Relative Motion Test Case.
Torus depiction and results of various representations.

Representing the torrus with 100 adjoining cylinders, the probability value was 0.067638. This is an overestimate of 2.3% and is in agreement with Patera. Because the tube bends towards the origin, the cylinders will overlap in regions of greater probability density and cause an overestimation. Representing the torrus with 100 sets of bundled parallelepipeds yielded more accurate results. Four such cases are displayed where the number of divisions per projected axis (face) were varied from 50 to 200; the latter produced a probability of 0.066178 (0.05% error) for 100 tubes. Increasing the number of divisions and/or number of tubes will yield even greater accuracy.

VII. Conclusion

Two methods were presented for determining collision probability in the presence of nonlinear relative motion. Both methods produced acceptable results with previously published test cases. The methods also incorporate dynamic covariance although no test cases could be found in the public literature with which to compare.

The first approach extends linear methods by representing the collision tube as a series of adjoining tubes in Cartesian space. The probability associated with the changing relative velocity direction is addressed because the collision tube is not straight, invalidating the simple dimensional reduction used for linear motion. Incremental limits of 100 seconds for maximum time step, one degree for maximum acceptable angle between adjoining tubes, and 0.25 σ for the maximum change in long-axis sigma for any tube were sufficient to achieve at least two significant figures of accuracy when calculating probability.

The second method represents the collision tube sections as bundles of abutting parallelepipeds to address the gaps and overlaps of the previous method. The probability of each is computed and summed to obtain the overall probability of an individual tube section and then all sections are summed. By creating a pixel file for each object as seen along the relative velocity vector, the files are merged to produce an overall pixel file that can represent any shape. Each pixel that contains a segment of the object becomes the face of another parallelepiped with the bundles forming compound miters.

In addition, two sequential tests were developed to determine if the linear assumption is valid for a specific conjunction. This was done by finding the minimum relative velocity needed for a user-specified tolerance and comparing to the actual relative velocity.

A MATLAB tool with Graphical User Interface was built that incorporates the methods and tests for spherical objects. The tool has been modified to incorporate pixel files of the actual shapes of the conjuncting objects.

References

[1]Foster, J. L., and Estes, H. S., "A Parametric Analysis of Orbital Debris Collision Probability and Maneuver Rate for Space Vehicles," NASA/JSC-25898, August 1992.

[2]Chan, K., "Collision Probability Analyses for Earth-Orbiting Satellites," Proceedings of the 7th International Space Conference of Pacific Basin Societies, Nagasaki, Japan, July 1997.

[3]Patera, R. P. "General Method for Calculating Satellite Collision Probability," *Journal of Guidance, Control, and Dynamics*, Vol. 24, No. 4, July-August 2001, pp. 716-722.

[4]Chan, K., "Improved Analytical Expressions for Computing Spacecraft Collision Probabilities," AAS Paper No. 03-184, AAS/AIAA Space Flight Mechanics Meeting, Ponce, Puerto Rico, 9-13 February 2003.

[5]Chan, K., "Short-Term vs Long-Term Spacecraft Encounters," AIAA Paper No. 2004-5460, AIAA/AAS Astrodynamics Specialist Conference, Providence, Rhode Island, 16-19 August, 2004.

[6]Alfano, S. "A Numerical Implementation of Spherical Object Collision Probability," *Journal of the Astronautical Sciences*, Vol. 53, No. 1, January-March 2005, pp. 103-109.

[7]Patera, R. P. "Calculating Collision Probability for Arbitrary Space-Vehicle Shapes via Numerical Quadrature," *Journal of Guidance, Control, and Dynamics*, Vol. 28, No. 6, November-December 2005, pp. 1326-1328.

[8]Alfano, S., "Review of Conjunction Probability Methods for Short-term Encounters," AAS Paper No. 07-148, AAS/AIAA Space Flight Mechanics Meeting, Sedona, Arizona, 28 January-01 February 2007.

[9]Chan, K., "Spacecraft Collision Probability for Long-Term Encounters," AAS Paper No. 03-549, AAS/AIAA Astrodynamics Specialist Conference, Big Sky, Montana, 3-7 August, 2003.

[10]Patera, R. P. "Satellite Collision Probability for Nonlinear Relative Motion,", *Journal of Guidance, Control, and Dynamics*, Vol. 26, No. 5, 2003, pp. 728–733.

[11]Alfano, S., "Addressing Nonlinear Relative Motion For Spacecraft Collision Probability," AIAA Paper No. 2006-6760, 15th AAS/AIAA Astrodynamics Specialist Conference, Keystone, Colorado, Aug 21-24, 2006.

[12]McKinley, D. P., "Development of a Nonlinear Probability Collision Tool for the Earth Observing System," AIAA Paper No. 2006-6295, 15th AAS/AIAA Astrodynamics Specialist Conference, Keystone, Colorado, Aug 21-24, 2006.

[13]Vallado, D. A., *Fundamentals of Astrodynamics and Applications*, 3rd ed., Microcosm Press, Hawthorne, California, and Springer, New York, New York, 2007, p. 796.

[14]Alfano, S. "Relating Position Uncertainty to Maximum Conjunction Probability," *Journal of the Astronautical Sciences*, Vol. 53, No. 2, April-June 2005, pp. 193-205.